

# Magnetic biomonitoring of roadside pollution in the restricted Midagahara area of Mt. Tateyama, Toyama, Japan

Kazuo Kawasaki<sup>1</sup>  · Keiji Horikawa<sup>1</sup> · Hideo Sakai<sup>1</sup>

Received: 17 March 2016 / Accepted: 27 February 2017 / Published online: 7 March 2017  
© Springer-Verlag Berlin Heidelberg 2017

**Abstract** Magnetic biomonitoring techniques and in situ top-soil magnetic susceptibility measurements have been shown to be rapid, cost-effective, and useful methods for investigating roadside pollution. However, combustible vegetation in samples makes it very difficult to use them in high-temperature magnetic experiments although the thermal alteration of spontaneous magnetization is a fundamental magnetic property and can be used to identify reliably the magnetic minerals. Here, we report the first magnetic biomonitoring results of dust deposited on plant leaves along the Tateyama-Kurobe Alpine route at the highly protected Midagahara wetland areas of Mt. Tateyama in Toyama, Japan. In-field magnetic susceptibility from 15 sites (161 points) shows higher susceptibilities near the roadside. Dust deposited on the leaves of *Sasa kurilensis*, or dwarf bamboo, has been wiped off at 12 sites (64 samples) with a commercial ethanol wipe sheet or silica wool damped in ethanol and subjected to rock magnetic analyses. Thermomagnetic remanence curves and low-temperature behaviors for samples collected near the roadside using silica wool show clearly that the main magnetic mineral in the dust is partially oxidized magnetite. Further, detailed rock magnetic analyses and elemental analyses of leaves in the study area indicate that (a) the magnetic mineralogy on leaves' surface is consistent throughout the study area and (b) higher saturation isothermal remanent magnetization intensities as well as higher concentrations of Pb, Fe, Cr, and Y are observed near the roadside, i.e., the closer to the roadside, the

more anthropogenic materials, including partially oxidized magnetite, are present. Also, microscopic observations show the lack of spherical grains, indicating that dust on the roadside leaves is derived from passing vehicle rather than industrial process. Both rock magnetic and geochemical results show that *S. kurilensis* would be an excellent candidate for investigating air pollution. Also, the proposed wiping-off method of collecting dust from plant surfaces is an effective non-destructive method that can be applied even in highly restricted collection areas, because detailed magnetic mineralogy, including superparamagnetic minerals, could be determined with the use of silica wool for use in both high- and low-temperature experiments.

**Keywords** Environmental magnetism · Oxidized magnetite · Roadside soil and dust on dwarf bamboo · National park · Japan

## Introduction

Dust from vehicles is a major source of roadside pollution. Dust particles from vehicles can range in diameter from 0.01 to 5000  $\mu\text{m}$  (Ninomiya et al. 1970); however, most urban road dust ranges from 3 to 100  $\mu\text{m}$  in diameter and dust from vehicle exhaust from 3 to 30  $\mu\text{m}$  (Thompson et al. 1984). Evans and Heller (2003) imply that the iron-rich magnetic material results from rusting of the bodywork, wear of the moving parts, and ablation from the interior of the exhaust system rather than from the fuel itself. Furthermore, these fine-grained dusts falling onto plants may block stomata and reduce photosynthesis (Farmer 1993). Also, substratum chemistry may be altered, causing changes not only to growth of vegetation but also to animal communities.

Environmental magnetic monitoring methods have been applied to various pollutions and shown as non-destructive,

Responsible editor: Philippe Garrigues

✉ Kazuo Kawasaki  
kkawasak@sci.u-toyama.ac.jp

<sup>1</sup> Section of Earth and Environmental Systems, University of Toyama, Toyama-shi, Toyama 930-8555, Japan

rapid, and cost-effective methods (e.g., Versteeg et al. 1995; Heller et al. 1998; Desenfant et al. 2004; Wang and Yong 2005; Karimi et al. 2011). This is because many industrial processes generate airborne magnetic materials, and therefore, magnetic data can be used as primary information of industrial contaminants. Topsoil magnetic susceptibility measurements have been shown to be highly useful for investigating the traffic pollutants along roadsides (e.g., Hoffmann et al. 1999; Schibler et al. 2002; Schmidt et al. 2005; Lu and Bai 2006; Canbay et al. 2010; Wang et al. 2013). Similarly, environmental magnetic studies on road dusts that have been directly collected by the ground sweeping method have been shown to be an effective method to determine the spatial and temporal distribution of anthropogenic materials (Kim et al. 2007, 2009; Yang et al. 2010). Recently, Bučko et al. (2011, 2013) reported environmental magnetic results for packed snow deposited along a roadside. They concluded that this snow provides an effective way to study the spatial distribution of pollution derived from passing vehicles. Atmospheric pollution related to traffic has been studied also by magnetic biomonitoring techniques using tree leaves (e.g., Schadlich et al. 1995; Matzka and Maher 1999; Pandey et al. 2005; Maher et al. 2008; Hansard et al. 2012; Rai 2013; Rai et al. 2014), tree bark (Kletetschka et al. 2003) and tree rings (Zhang et al. 2008). Recently, Hofman et al. (2013) showed that biomagnetic monitoring using tree leaves can be used to assess small-scale spatial distribution of atmospheric dust based on different tree crowns with various heights. In most such studies of vegetation, leaves are removed and studied directly in the laboratory although Flanders (1999) reported that wiping off the surface would be an effective method to study fly ash from fossil fuel power stations. Magnetic properties of such vegetation are often determined by a combination of susceptibility, hysteresis parameters, isothermal remanent magnetization (IRM), and/or anhysteretic remanent magnetization (ARM). Zhang et al. (2008) conducted low-temperature experiments on tree bark and tree trunk samples collected near a smelting factory in China and found pseudosingle (PSD) to multidomain (MD) magnetite as well as superparamagnetic (SP) magnetite in them. Despite the fact that thermomagnetic measurements of the high-temperature dependence of saturation magnetization and/or magnetic susceptibility are fundamental and effective methods to determine magnetic mineralogy, vegetation samples contain combustible organic components, and so, these techniques are generally avoided. In this study, we have met our first objective and report the first thermomagnetic remanence curves for dust deposited on plant leaves along a roadside.

Few systematic magnetic investigations on the spatial distributions of such roadside pollution have been reported in Japan (Kawasaki et al. 2015). This deficiency is due to (a) lots of active volcanoes in Japan that supply great amounts of magnetically enhanced fly ash and (b) the dense population

in Japan that causes a substantial amount of magnetic noise (Torii 2005). Hence, the magnetic investigation of topsoil for the spatial distribution of pollution may not become a conventional method throughout Japan or similar volcanic region. Conversely, plant leaves are likely less affected by volcanic ash and/or background geology. Our second objective is to demonstrate the efficiency of using magnetic biomonitoring methods in Japan, especially at a highly protected area, based on magnetic data, including in-field susceptibility measurements and in-laboratory rock magnetic measurements, as well as elemental data and microscopic observation. Magnetic methods can only detect magnetic minerals in samples so that subsequent geochemical analysis and microscopic characteristics of the samples are conducted to evaluate if the observed magnetic data can be used as proximal information for identifying the source and concentrations of heavy metals in the study area.

## Study area

Mt. Tateyama, 3035 m in elevation, is a part of the Chubu Sangaku National Park in Japan, which is located in northern part of the Northern Japanese Alps (Fig. 1). The studied Midagahara areas are between ~1600 and ~1900 m in elevation. They became part of the Ramsar Convention on Wetlands of International Importance, especially as a Waterfowl Habitat in 2012. Mt. Tateyama is known as one of the three sacred mountains in Japan, and thus, the area has been relatively undisturbed since ancient times. In addition, the studied area is designated as a Special Protection Zone and is restricted to vehicular traffic and other constructions. The Tateyama-Kurobe Alpine sightseeing route is the only available road at Mt. Tateyama. The road is open from mid-April to the end of November when it is closed because of the heavy winter snowfall. The route is travelled mostly by a considerable number of non-hybrid buses as well as utility vehicles that maintain facilities for tourists and for construction (Kume et al. 2009). The number of vehicles is recorded by the Toyama prefecture's public road corporation. In 2014, 30,976 tourists and transit buses used the road. The maximum uses of leaded gasoline were during 1960–1965 in Japan. Horikawa et al. (2013) reported that the amount of lead observed in the Tateyama cedar tree is rapidly reduced after early 1980s in the Mt. Tateyama region.

Kawano (1999) reported that the highland wetlands at Mt. Tateyama, including Midagahara area, were significantly damaged by the construction of the Alpine route and hotels between 1956 and 1964, especially in 1963 and 1964. The effects of passing vehicles on the surrounding environment have been reported for the Bijyodaira forest area at Mt. Tateyama, which is about 1000 m below the Midagahara wetland area, by Kume et al. (2009). They examined the decline

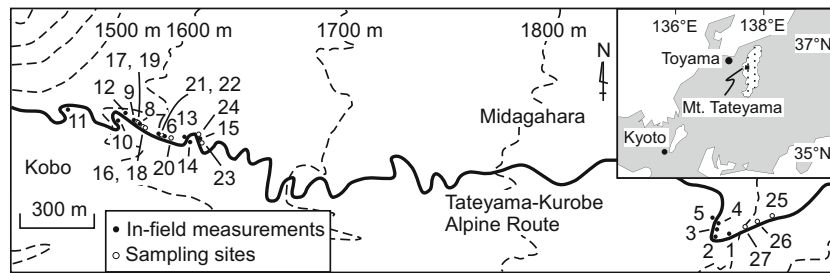


**Fig. 1** A regional map of the Midagahara area with the locations of the in-field susceptibility survey sites (black circles) and sampling sites (white circles). Note the dashed area on small inlet shows the Northern Japanese Alps, which is designated as the Chubu Sangaku National Park

of *Fagus crenata*, or Japanese beech, trees along the route between 1999 and 2006. They found that the decline was not caused significantly by air pollution emitted from the passing vehicles but rather that tree damage and death were caused mostly by regional and long-range transboundary air pollution. Horikawa et al. (2013) reported evidence of historical changes in soil acidification around a Tateyama cedar tree in the Bijyodaira area, which they related to significant increases of Ca concentrations that accompanied the local road building activities. Recently, Kawasaki et al. (2015) reported results of an environmental magnetic study of roadside contamination in the Bijyodaira forest area, and they concluded that anthropogenic magnetite as well as heavy metal concentration such as Zn has been deposited mainly within ~2 m of the Alpine road route.

**Methods and results**

**In-field measurements**

In-field volume susceptibility was measured using a Bartington MS2-D susceptibility meter with a probe that can reach to a depth of 10 cm (Lecoanet et al. 1999). At each measurement point, five measurements were done to ensure repeatability and consistency. Also, air measurements were made before and after each measurement to ensure compensation for instrument drift. The in-field susceptibility was measured at 15 sites along the Tateyama Kurobe Alpine route from the Kobo area to the Midagahara area (Fig. 1). No precipitation was observed at the studied area for at least 3 days before in-field surveys and samplings. A survey line was set up with various lengths from the road (Table 1). Note that the 0 m point at each site is set at 0.3 m from the roadside gutter to avoid the effect of its extremely high susceptibility. The spacing of survey points along each line was set in four intervals in order to determine the spatial distribution of pollution related to vehicles: (a) 0.25 m spacing between 0 and 1 m, (b) 0.5 m spacing between 1 and 5 m, (c) 1 m spacing between 5 and 10 m, and (d) 5 m spacing between 10 and 30 m (Fig. 2).

In-field susceptibility values vary by two orders of magnitude, ranging from  $2.4 \times 10^{-5}$  to  $351.6 \times 10^{-5}$  (SI). The

median susceptibility of all measurements points ( $N = 161$ ) is  $19.0 \times 10^{-5}$  (SI) (quartiles:  $Q_1 = 9.0 \times 10^{-5}$ ,  $Q_3 = 47.8 \times 10^{-5}$ ). Higher susceptibility values than the median susceptibility were mostly observed within 1 m from the roadside, except at sites 5 and 6 (Fig. 2). In addition, the susceptibility decay curves of all sites except site 5 show rapid decreases within 2 m from the roadside. High susceptibilities between 2 and 5 m at site 5 are likely due to rock fragments, and therefore, the result of site 5 is excluded from the following discussion.

**Sampling and initial susceptibility measurements**

The study area is part of the Special Protection Zone of the Chubu Sangaku National Park in Japan. Therefore, collecting natural resources such as rocks, soils, plants, and tree leaves are strictly prohibited in the area and permission is required to collect such samples. Hence, non-destructive collecting methods are required to study the details of the spatial distribution of roadside pollution. In this study, the materials deposited on the leaves of *Sasa kurilensis*, or dwarf bamboo, near the roadside have been collected by two different

**Table 1** In-field magnetic susceptibility survey lines

Sites	Length from the road (m)
1	5
2	20
3	5
4	30
5	10
6	15
7	10
8	10
9	10
10	5
11	5
12	5
13	4
14	15
15	5

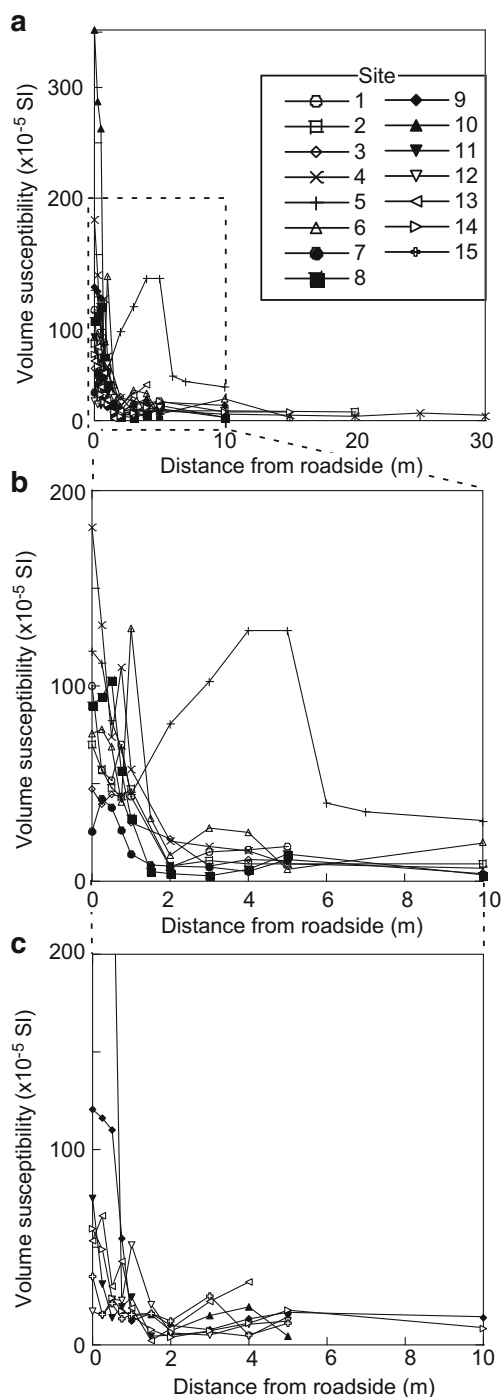


**Fig. 2** In-field volume susceptibility curves for **a** all survey lines, **b** sites 1–8 within 10 m from roadside, and **c** sites 10–15 within 10 m from roadside. Legends on **b**, and **c** are same as the ones on **a**

sampling methods to investigate their magnetic properties; i.e., the materials were wiped off with (a) a sheet of commercial ethanol wipe paper having with a width of 19.4 mm and a height of 13.2 mm for conventional environmental magnetic analysis and (b) a silica wool damped by ethanol for hysteresis loops and high- and low-temperature experiments. Because this method does not involve collections of actual plant leaves,

permission is not required. The dwarf bamboo's leaf generally has an oval shape. A leaf with a major axis of  $\sim 10$  cm and a minor axis of  $\sim 3$  cm in length at a height of  $\sim 0.5$  m from the ground level was selected for this study. Ten such leaves were wiped off with a single wipe sheet so that each sheet sample contains the sum of ten leaves' dust. The sample collection was done at 12 sites that are located near the in-field measurements (Fig. 1), resulting in 64 samples in total. Flanders (1999) proposed the use of a paper tissue or towel that is then rinsed in water. The magnetic materials were caught with a powerful permanent magnet. Here, we directly put the “dirty” wipe sheet into a  $7\text{ cm}^3$  non-magnetic plastic cubes to measure its magnetic properties, because the use of a magnet after rinsing out the samples highly likely misses the non-magnetic superparamagnetic minerals as well as other weak magnetic minerals that might be in samples such as hematite. All magnetic measurements were conducted in the rock magnetic laboratories at the University of Toyama. Further, dust samples collected by a wipe sheet were also used for scanning electron microscope (SEM) observation and for electron probe micro analyzer (EPMA) measurements.

Low-field volume susceptibility ( $k$ ) was measured with an Agico KLY3CS3 Kappabridge, and these values were divided by mass to calculate the mass susceptibility ( $\chi$ ). The median mass susceptibility of all 64 specimens is  $-2.27 \times 10^{-6}$  ( $\text{m}^3/\text{kg}$ ) ( $Q_1 = -3.03 \times 10^{-6}$ ,  $Q_3 = -1.60 \times 10^{-6}$ ), which is not significantly different from the mass susceptibility of unused wipe sheet of  $-2.56 \times 10^{-6}$  ( $\text{m}^3/\text{kg}$ ). The results indicate that the susceptibilities of any magnetic minerals deposited on the leaves are too low to measure.

### Saturation IRM

The relative amounts of magnetic minerals as well as the magnetic mineralogy and their effective domain size were tested using stepwise isothermal remanent magnetization (IRM) acquisition analysis of 13 specimens from sites 19, 21, 23, and 27, i.e. 4 specimens from the 0 m locations; 4 specimens from the 2 m locations; 1 specimen from the 6 m location; 3 specimens from the 10 m locations; and 1 specimen of an unused sheet of wipe paper. The IRM analyses were done using a Magnetic Measurements PM9 pulse magnetizer to magnetize each specimen in 11 direct current (DC) field steps up to 900 mT. The value of  $0.9 \times J_{900}$  is used here as saturation where  $J_{900}$  is the maximum remanence, saturation IRM (SIRM), and intensity at 900 mT. The specimens were subsequently alternating field (AF) demagnetized in ten steps up to 80 mT. The rapid acquisition of IRM to saturation at 150 mT for all specimens including the unused wipe sheet is typical of MD magnetite (Fig. 3) (Symons and Cioppa 2000). The averaged SIRM intensities normalized by leaf area are  $248 \times 10^{-7}$  ( $\text{A} = \text{Am}^2/\text{m}^2$ ) at the 0 m locations,  $85.9 \times 10^{-7}$  (A) at the 2 m locations,  $51.9 \times 10^{-7}$  (A) at the 6 m location, and  $28.1 \times 10^{-7}$

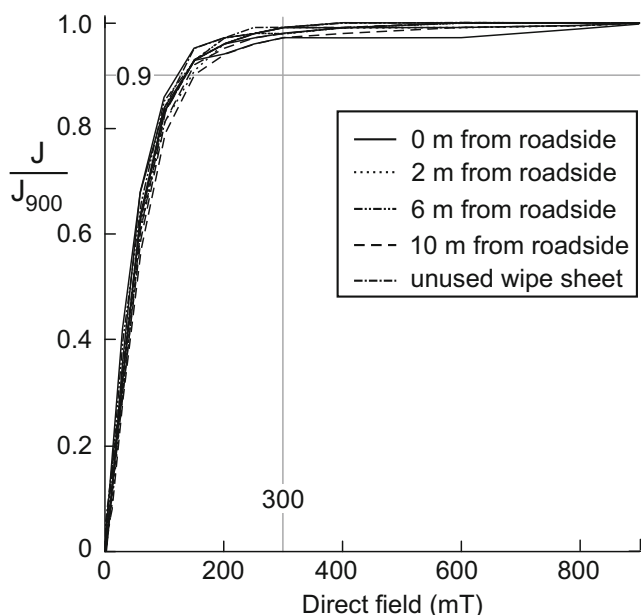


**Fig. 3** IRM acquisition curves for selected samples taken from 0, 2, 6, and 10 m from roadside and an unused wipe sheet, showing little difference between samples.  $J_{900}$  means the intensity value at 900 mT

(A) at the 10 m locations. The SIRM intensity of unused wipe sheet is  $6.14 \times 10^{-7}$  (A), which is  $\sim 1/5$ th of the SIRM intensities at the 10 m locations, indicating that the effect of wipe sheet itself is minimal (Fig. 4).

Based on the initial test results, the rest of specimens were given an IRM at 900 mT; then, the DC field direction was reversed and the specimens were given an IRM at 300 mT (IRM<sub>-300</sub>) to measure the S-ratio of the specimens. The S-ratio ( $S_{300}$ ), which can vary from 0 to 1, is calculated according to Bloemendal et al. (1992):  $S_{300} = \{-(IRM_{-300} - SIRM) + 1\}/2$ . The S-ratio provides a measure of the relative amount of high-coercivity antiferromagnetic minerals to low-coercivity ferromagnetic minerals; i.e., higher  $S_{300}$  values reflect higher proportions of low-coercivity ferromagnetic minerals to high-coercivity minerals. The averaged S-ratio value of all 64 specimens is  $0.99 \pm 0.01$  (Table 3), indicating that the predominant magnetic minerals in the roadside dust are low-coercivity ferromagnetic minerals and not likely to be significantly different among the specimens. In other words, the magnetic mineralogy is likely similar regardless of the distance from roadside.

Based on the results of stepwise IRM acquisition tests and S-ratio, magnetic minerals of all specimens are likely to have the same PSD-MD magnetite-like phase, indicating that the SIRM intensity can be used as a proxy of the relative amounts of magnetic minerals. The SIRM intensities show progressively higher intensities on going closer to the roadside (Fig. 4), which is similar in trend to the in-field volume susceptibility results. This result indicates that higher susceptibility values observed for the in-field topsoil measurements were not caused by the higher susceptible gravels and were caused by dust from road.

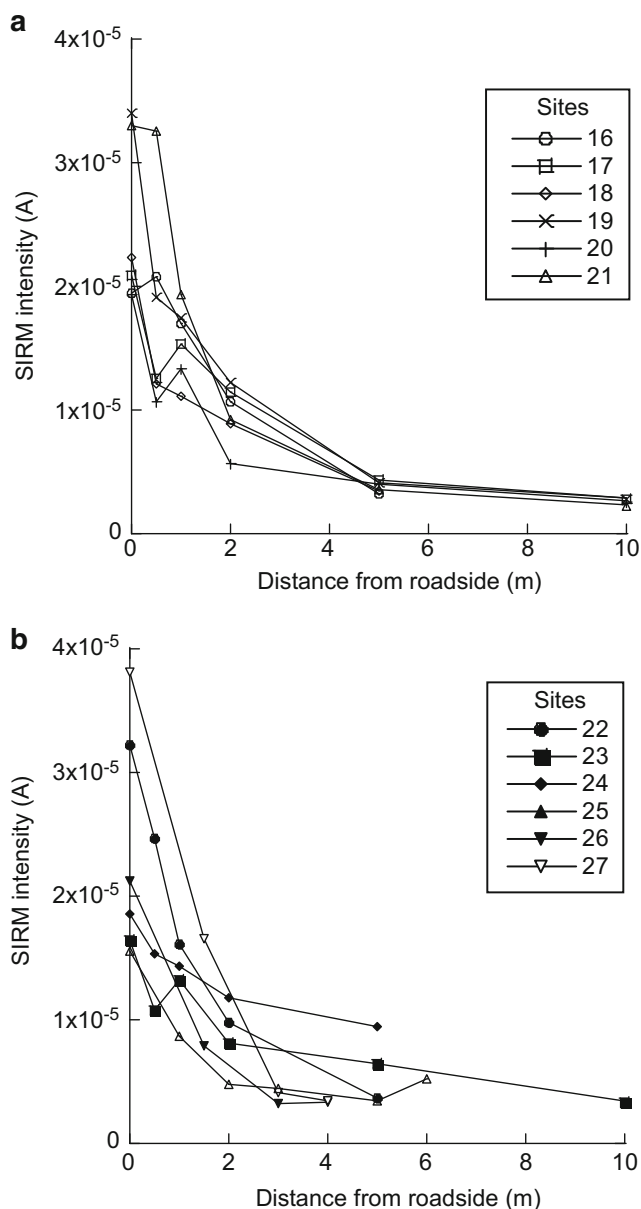


**Fig. 4** SIRM intensity curves for dust samples collected by wiping off the leaves' surfaces. **a** Sites 16–21. **b** Sites 22–27

### Hysteresis loops

From hysteresis loops and backfield demagnetization curve measurements, a saturation remanent magnetization ( $M_{rs}$ ), saturation magnetization ( $M_s$ ), coercivity ( $H_c$ ), and coercivity of remanence ( $H_{cr}$ ) can be obtained. Two ratios,  $M_{rs}/M_s$  and  $H_{cr}/H_c$ , are illustrated on a Day plot that allows the ferrimagnetic grain size to be estimated (Day et al. 1977; Dunlop 2002a, b). Hysteresis loops are generated by subjecting a sample to a direct magnetic field of 500 mT and by backfield demagnetization as well as by stepwise IRM acquisition tests up to 900 mT. The data were obtained for selected specimens using a Lake Shore Cryotronics PMC MicroMag vibrating



sample magnetometer (VSM) model 3900-04. The averaged value of three measurements was used to determine a sample's hysteresis loop. The observed diamagnetic component after  $\sim 100$  mT of the sample taken at 0 m location is likely caused by the sample holder and/or silica wool used for dust collection (Fig. 5a). The hysteresis loops of samples at  $>4$  m from roadside showed almost diamagnetism, indicating that there are few magnetic minerals in the dust (Fig. 5b). Such hysteresis loops were too noisy to determine the necessary  $M_{rs}/M_s$  and  $H_{cr}/H_c$  values after paramagnetic/diamagnetic correction, and therefore, these data are not subjected to the Day plot analysis. On a Day plot, most data points show an elongated distribution within the PSD region (Fig. 6), indicating that each sample contains a mixture of SD and MD particles rather than PSD grain size only (Evans and Heller 2003).

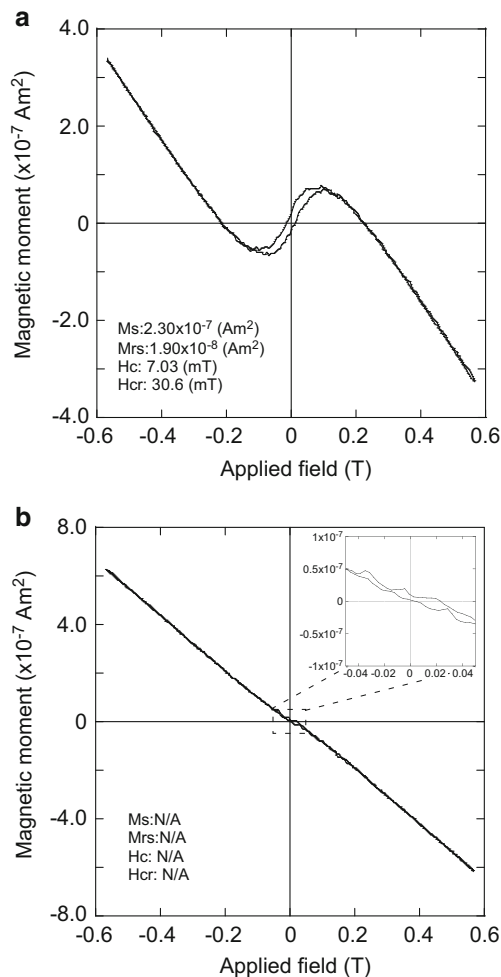


**Fig. 5** Hysteresis loops for selected samples: **a** 0 m from roadside and **b** 10 m from road side at site 17. The small inlet of **b** is the enlarged view between 50 and  $-50$  mT. The observed values after diamagnetic/paramagnetic correction for **a** specimen are  $M_s = 2.30 \times 10^{-7} \text{ Am}^2$ ,  $M_{rs} = 1.90 \times 10^{-8} \text{ Am}^2$ ,  $H_c = 7.03 \text{ mT}$ , and  $H_{cr} = 30.6 \text{ mT}$ . Note that  $H_{cr}$  value is observed by backfield measurement. Hysteresis parameters,  $M_s$ ,  $M_{rs}$ ,  $H_c$ , and  $H_{cr}$ , for **b** are not available (N/A) due to too weak magnetization

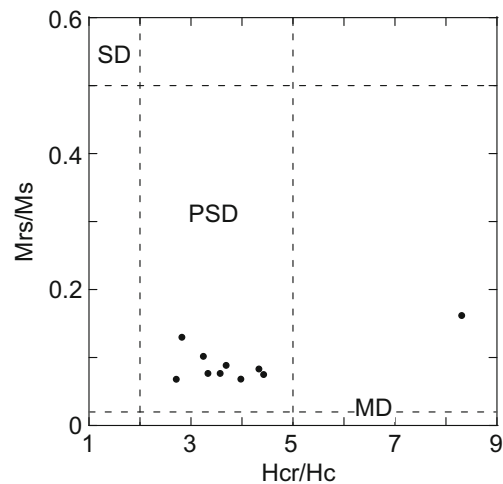
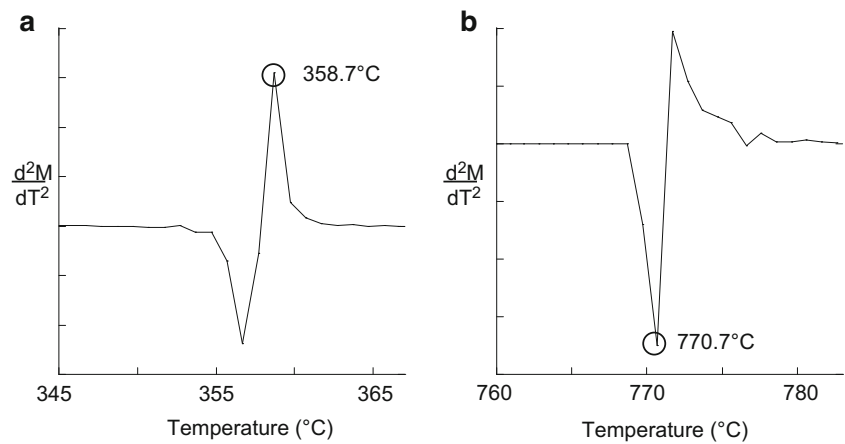


**Fig. 6** Day plots for selected samples

### Thermomagnetic curves

Thermomagnetic curves were obtained in the temperature range from 30 to 680 °C using the vibrating sample magnetometer (VSM) in a He atmosphere under 100 mT DC field. Since the wipe sheets used for dust collections are flammable, silica wool damped by ethanol was used to collect dust on leaves at study area for thermomagnetic experiments. Thermomagnetic experiments have been carried out with helium gas rather than conventional argon gas. Helium gas has much higher thermal conductivity than argon gas, which helps the samples to quickly reach the setting temperature in the furnace. In addition, the pause length after each temperature increment is set at 5 s between 30 and 600 °C and 10 s between 600 and 680 °C, respectively, with 1 °C temperature increment. These settings minimize unwanted thermal lags in the specimen (Fig. 7) although one cycle of the thermal experiment from the 30 to 680 °C heating process and back down from 680 to 150 °C takes  $\sim 2.5$  h. Each Curie temperature is estimated by following the differential method of Tauxe (1998), which seeks the peak of data by differentiating twice. The differential method is easier to calculate with a computer although the determined Curie temperature seems to be slightly lower than the Curie temperature determined using the intersecting tangent method of Grommé et al. (1969). A well-defined Curie temperature was observed 595 °C for the 0 m samples from the roadside (Fig. 8a–c), which identifies maghemite as the predominant magnetic mineral. Conversely, the samples were collected from further than 4 m from the roadside fall to give an obvious Curie temperature because of the interference from noise caused by trace amounts of magnetic minerals although the rough Curie temperature is also around 600 °C (Fig. 8d, e). The reversible thermomagnetic curves indicate that there was little inversion from maghemite to hematite during the heating experiments (Fig. 8a).

**Fig. 7** Thermomagnetic remanence curves after two differentiations for Ni/Fe standard. Note that the observed Curie temperatures on **a** Ni and **b** Fe are very close to the Curie points of Ni (358 °C) or Fe (770 °C)



The low-temperature behaviors of the dust samples were measured for further identification of magnetic minerals. Two samples taken at 0 m distance from the roadside at sites 20 and 23 were subjected to the low-temperature measurements using a Quantum Design magnetic property measurement system (MPMS) XL. Each sample was magnetized in 150 mT DC field at 5 K and monitored during zero-field heating to 300 K. Magnetization decreases rapidly from 5 to ~45 K and then decreases weakly to moderately around ~95 and ~110 K for sites 20 and 23, respectively (Fig. 9), indicating that the main magnetic minerals in the dust on the leaves are oxidized magnetite rather than magnetite (de Boer and Dekkers 1996; Dunlop and Özdemir 1997; Kosterov 2003).

Based on the thermomagnetic curves, the main magnetic mineral in the dusts on leaves is likely oxidized magnetite or magnetite with the presence of maghemite. The determination of the Curie temperature for maghemite is generally difficult due to its metastability; i.e., maghemite has a strong tendency to convert into hematite at temperatures greater than 430 °C (e.g., Banin et al. 1993; Dunlop and Özdemir 1997; Gehring et al. 2009). However, the thermal stability of maghemite from either basaltic rocks, loess sediments, or an iron ore is reported to be at ~600–610 °C (de Boer and Dekkers 1996; Spassov et al. 2003; Chevrier et al. 2006). Here, our thermomagnetic experiments for the dust on leaves collected by silica wool with ethanol clearly identify the magnetite with the presence of maghemite rather than magnetite only without conversion into hematite (Fig. 8). In addition, the low-temperature behavior of dust samples showed smaller decrease of magnetization than previously reported results from polluted tree wood (Zhang et al. 2008) in a wider temperature range from 95 to 115 K, indicating that the dominant magnetic mineral is oxidized magnetite (Fig. 9). Also, the relatively rapid decreases of remanence from 2 to 50 K indicate the presence of SP grain (Lovley et al. 1989). These results indicate that wiping off a leaf’s surface with silica wool can be an effective method to collect and then identify the magnetic minerals using high- and low-temperature experiments. In addition, our results show that

titanomagnetite found in the soils at the Bijyodaira area (Kawasaki et al. 2015) is not observed in the dusts on the leaves, indicating that these dusts have not been significantly contaminated by dust from the weathering of the bedrocks. Thus, leaf dust is an excellent candidate for studying the distribution of anthropogenic pollutants along the roadside.

The identification of the magnetic minerals derived by vehicular exhaust is a controversial problem. Based on Mössbauer studies, the major magnetic mineral of atmospheric particles collected with stational particle matter collectors is either maghemite or partially oxidized magnetite (Tong et al. 2001; Muxworthy et al. 2002, 2003; Petrovský et al. 2013). Similarly, high- and low-temperature behaviors of street dusts collected by a plastic hand broom in China showed that the main magnetic mineral of such dust is MD magnetite with the presence of maghemite and Fe particle, although these dusts are likely delivered from various anthropogenic activities such as vehicular traffic, residential fossil fuel burning, and smelting plant (Zhang et al. 2012). Conversely, magnetic minerals of atmospheric particles directly collected from automobiles include magnetite, goethite, or hematite rather than maghemite (Weber et al. 2000). Therefore, Muxworthy et al. (2002) inferred that the different sampling strategy may cause different magnetic mineralogy. The main difference between stational collectors and direct sampling is time. In this study, the plant leaves worked similarly to stational collectors and the observed thermomagnetic curves show clearly the presence of either maghemite or partially oxidized magnetite. Iron particles would easily oxidize to maghemite while resting on the leaves for many weeks being exposed to weathering. Therefore, the dominant magnetic mineral of our dust samples is likely magnetite with the presence of a superficial maghemite layer.

### Geochemical analysis of bulk leaves

We collected leaves of the *S. kurilensis* at sites 25, 26, and 27 to measure trace metal concentration in bulk leaves (Fig. 1).

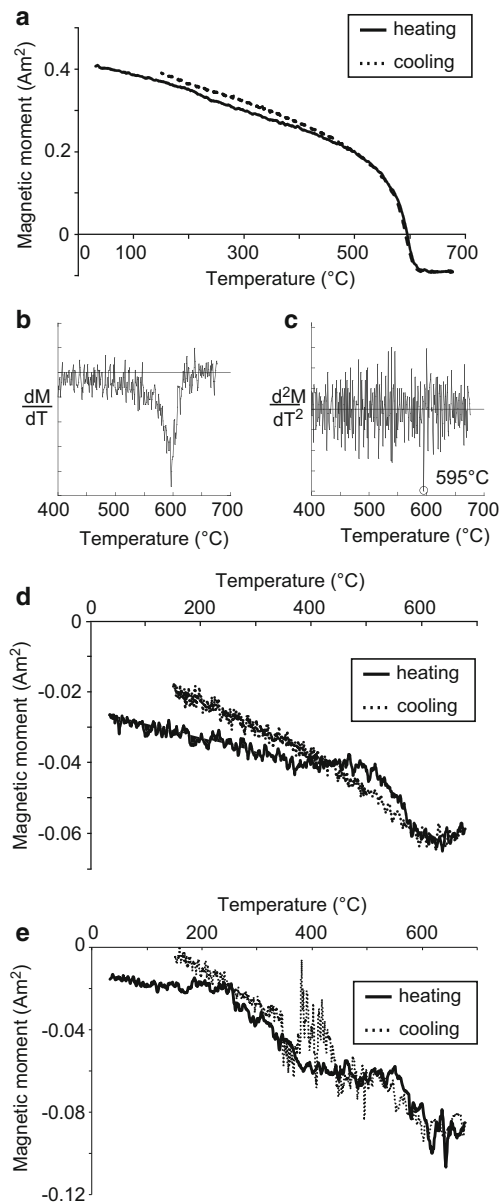


**Fig. 8** Thermomagnetic remanence curves, for example, samples **a** 0 m at site 27, **b** data **(a)** after one differentiation, **c** data **(a)** after two differentiations, **d** 6 m at site 27, and **e** 4 m at site 26. Solid and dashed lines show heating and cooling curves, respectively. The curves were measured with the samples in a He atmosphere under 100 mT DC field using a simple moving average (number of readings  $n = 5$ ). Note that the negative magnetic moment offsets in **a**, **d**, **e** are caused by the diamagnetic silica wool that is used for collecting the dust

The central parts of each leaf were used for the geochemical analysis. The dried leaf samples of ~50–100 mg each were digested in 5 mL of trace metal grade concentrated  $\text{HNO}_3$  and 0.1 mL trace metal grade concentrated HF (TAMAPURE AA-100 from Tama Chemical Ltd., respectively) under reflux at 70–120 °C for 3 h and then dried at 130 °C. These samples were diluted with 2%  $\text{HNO}_3$  for measurement. Elemental analysis was performed by an ELEMENT 2 (Thermo

Scientific) sector field inductively coupled plasma-mass spectrometer (SF-ICP-MS).

We measured Fe, Pb, Cr, Y, Cu, and Cd concentrations in bulk leaf samples for six samples at three sites (Table 2). Metal concentrations were determined by internal standard (Rh and Bi) calibration, and calibration standards were prepared from a certified reference material of JB-1a (Geological Survey of Japan (GSJ)) at five concentration levels. The correlation coefficient ( $r$ ) values of each element calibration curve were more than 0.99.

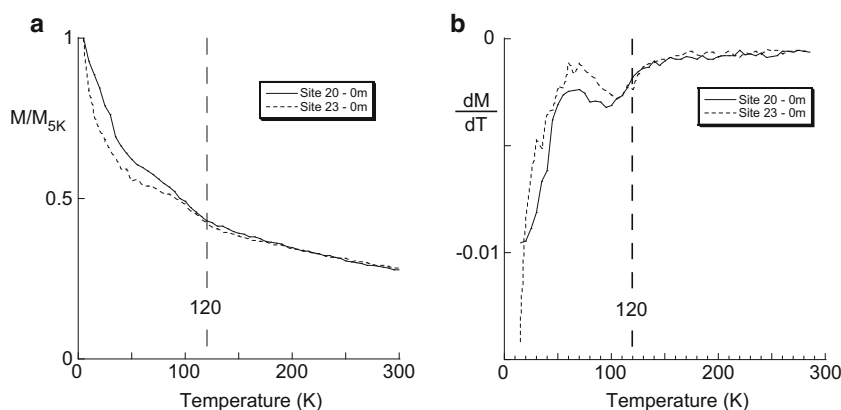
Even though the number of the geochemical data for bulk leaf samples is not sufficient to discuss the details of heavy metal contents, there was the robust trend that Fe, Pb, Cr, and Y concentrations were consistently higher in the leaves of the *S. kurilensis* grown near roadside compared to the locations 4–6 m away from the roadside (Table 2). Further, Pb/Fe ratios, indication of the relative amounts of Pb against Fe, show consistently higher values near roadside compared to the locations 4–6 m away from the roadside, indicating that Pb was more concentrated in the leaves of the *S. kurilensis* grown near the roadside than Fe. Maher et al. (2008) reported environmental magnetic results combined with geochemical analyses of birch leaves in Norway and found that the SIRM values and leaf Pb concentrations show stronger correlation than the Pb and Fe correlation. They concluded that Pb is associated with the magnetic Fe particulates that arise from vehicle combustion/exhaust processes rather than vehicle ablation or abrasion. Although our bulk data cannot discriminate the contribution of those metals from soil and dust deposited on the leaf surface, the observed data clearly show that the roadside environments are exposed to traffic pollutant.

### Microscopic characteristics

Scanning electron microscope (SEM) observations were performed on the magnetic extracts from the dirty wiper sheets to identify the magnetic materials derived from passing vehicles. The magnetic extracts were collected by a neodymium magnet because a sheet of ethanol wipe paper is easily dried up, and the materials on the wipe paper smoothly come out. The compositions of magnetic extracts were determined using a JEOL JXA-3230 electron probe micro analyzer (EPMA). The SEM observations were obtained using either a Hitachi Miniscope TM3030 or EPMA. Microscopy analyses of 26 grain samples reveal basically one morphology of grains, angular/aggregate particles that have diameters of ~5–150  $\mu\text{m}$  (Fig. 10). The EPMA analyses of 19 points showed a variety of chemical compositions (Fig. 10), such as C, O, Fe, Al, Cu, Zn, Ti, Ni, Ca, B, Na, V, Mg, P, K, Cl, Co, Mn, Pb, and Si. The results indicate that the elements distributed heterogeneity on the grains. However, C, Fe, O, and Al are found on all 19 analyzed areas, suggesting that these elements are abundant and present universally on the study areas. The presence of Fe and



**Fig. 9** **a** Low-temperature curves, for example, samples at 0 m distance from roadside from sites 20 and 23. **b** The low-temperature curves after one differentiation for the data (**a**). The IRM intensities at 5 K for sites 20 and 23 are  $6.71 \times 10^{-4}$  ( $\text{Am}^2/\text{kg}$ ) and  $4.90 \times 10^{-4}$  ( $\text{Am}^2/\text{kg}$ ), respectively



O on all analyzed area indicates that the most angular/aggregate particles in the dust contain iron oxides.

**Discussion**

Observed in-field volume susceptibilities rapidly decrease with the distance from the roadside. This is similar in trend to the leaves’ SIRM intensities. Further, the geochemical analysis of the leaves shows that Fe, Pb, Cr, and Y concentrations that were used in a wide variety of car materials, such as bodywork, brake system, and catalytic converter, were consistently higher in the leaves of the *S. kurilensis* grown near roadside compared to the locations 4–6 m away from the roadside (Table 2). Unlikely the Fe, Pb, Cr, and Y concentrations, Cu and Cd concentrations increase with the distance from the roadside. These elements can be either industrial or natural in origin. Herawati et al. (2000) reported the Cu and Cd levels in soil in Japan, including Hokuriku district where the study area is located, China, and Indonesia. They found higher Cu and Cd values in Japanese soil and suggested that the historical mines in Japan would likely have a significant impact on soils. These Cu and Cd elements might have delivered by passing vehicles in the past or regional transportation from near historical mines such as the Kamegai deposit that is located about 14 km SW of the study area and was active between 1567 and 1926. These elements were likely remnant after being washed away by

rain, and therefore, they do not show similar in trend to the other heavy metals or magnetic properties.

The SEM observations show that the major morphology of grain is angular/aggregate particles. The lack of spherical grains implies that the dusts on the roadside leaves are likely derived from vehicle emissions rather than industrial processes (Kim et al. 2009; Bućko et al. 2010). The non-spherical particles can be generated via exhaust emissions, braking systems, and abrasion or corrosion of engine and body material (Matzka and Maher 1999; Lu et al. 2011). These materials contain magnetite-like particles that are agglomerated with Cu, Pb, and Zn (Hoffmann et al. 1999; Bućko et al. 2010). The EPMA analysis indicates that Fe and O are distributed universally in the samples, suggesting that Fe can be candidates as a trace element for pollution investigation in this study area; i.e., the use of iron oxide minerals is reasonable for monitoring regional pollution in the area.

The observed susceptibilities and SIRM fluctuations are consistent with the mass susceptibilities as well as with the heavy metal contents in the topsoil of the Bijyodaira forest area at Mt. Tateyama as reported by Kawasaki et al. (2015). This result indicates that the in-field susceptibility measurements on a wetland area are an effective method to provide primary information on the distribution of roadside dust without any surface destruction in the Mt. Tateyama region. In addition, the SIRM intensities show more clearly the intensity decay distribution from the roadside than do the observed in-field susceptibilities or the mass susceptibilities at Bijyodaira,

**Table 2** Heavy metal concentrations of *Sasa kurilensis* leaves from selected sites

Sites	Distance from roadside (m)	Fe ( $\mu\text{g}/\text{g}$ )	Pb ( $\mu\text{g}/\text{g}$ )	Cr ( $\mu\text{g}/\text{g}$ )	Y ( $\mu\text{g}/\text{g}$ )	Cu ( $\mu\text{g}/\text{g}$ )	Cd ( $\mu\text{g}/\text{g}$ )	Pb/Fe
25	0	148.68	0.65	0.372	0.022	5.444	0.026	4.372E-03
25	4	119.05	0.20	0.257	0.011	7.094	0.020	1.714E-03
26	0	199.29	0.51	0.444	0.025	7.070	0.008	2.572E-03
26	4	156.39	0.40	0.304	0.021	7.654	0.010	2.531E-03
27	0	217.06	1.17	0.502	0.026	5.355	0.007	5.372E-03
27	6	177.66	0.37	0.376	0.020	7.220	0.026	2.058E-03

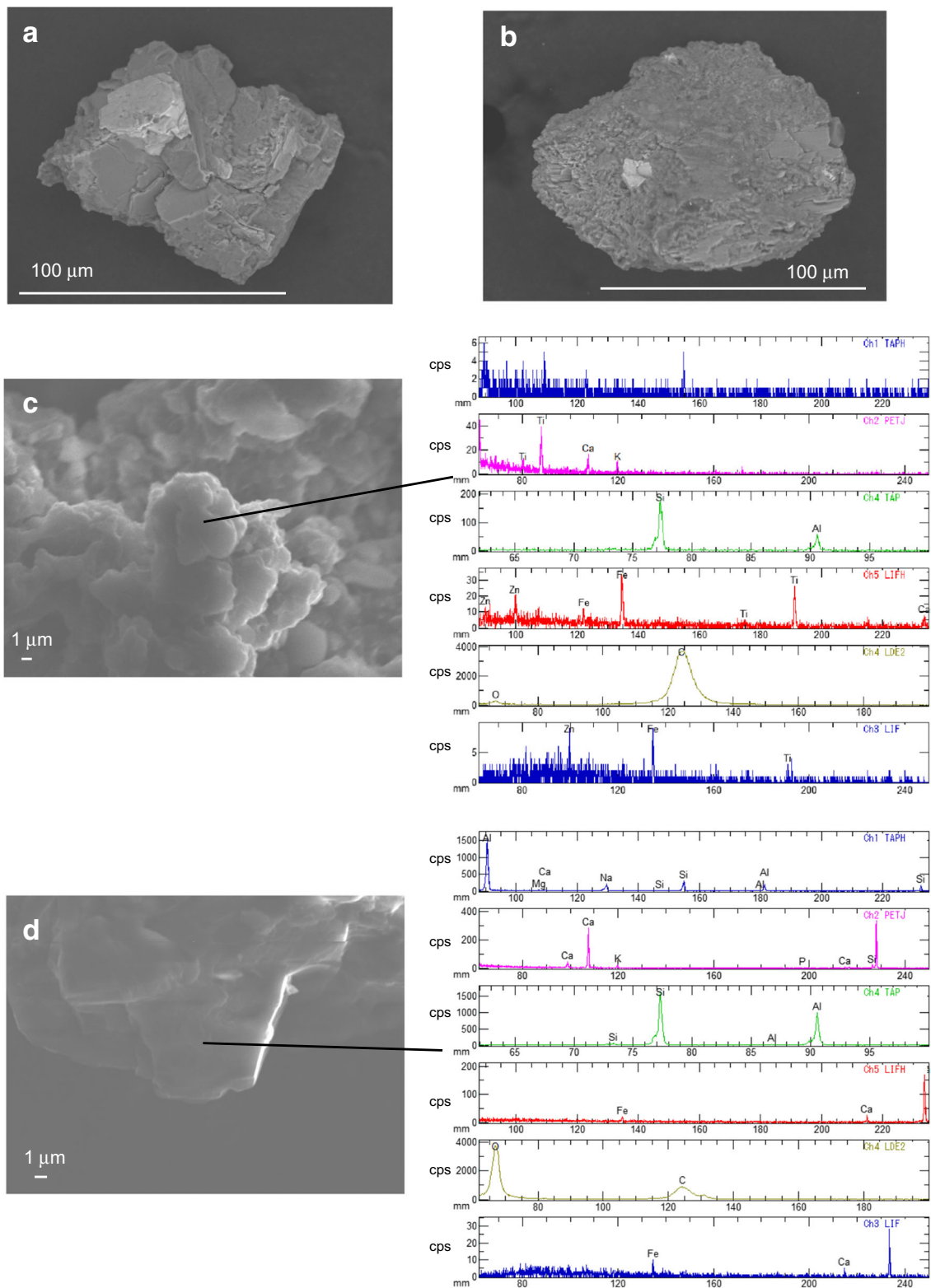


**Fig. 10** Representative results of SEM photographs (a, b) and EPMA spectra (c, d) of magnetic particles separated from selected dust samples

indicating that the leaves of the *S. kurilensis* are less affected by the regional geology than topsoil.

Based on thermomagnetic remanence curves, low-temperature behaviors, and SIRM acquisition tests, the main

magnetic minerals in the leaf dust are oxidized magnetite. Day plots for the leaf dust fall in the PSD magnetite range. However, the hysteresis values of maghemite or oxidized magnetite do not differ seriously from those of magnetite of

similar grain size (Dunlop 2002b). The S-ratios are almost same value for all specimens and nearly 1.0, indicating that the magnetic minerals are likely consistent not only from site to site but also by distances from the roadside (Table 3). The crossover point of the SIRM acquisition and subsequent AF demagnetization curves yields a unique point for each sample that provides additional magnetic information (Symons and Cioppa 2000). All observed crossover points fall on similar region on PSD-SD magnetite/maghemite area (Fig. 11). In details, the samples taken at 0 m from roadside fall on PSD-SD region, samples taken at 10 m from roadside fall on SD region, and samples taken at 2 m from roadside fall on the middle of these two sets, indicating that the closer to the road, the coarser the oxidized magnetite present. In other words, magnetic grain size decreases with distance from the road. Therefore, it is likely that the dusts on the leaves in our study area are derived from the same source, which is probably the exhaust of passing vehicles.

The results of rock magnetic analysis, morphology, and elementary analyses demonstrate that (a) the leaves of the *S. kurilensis* plant near roadside are a good candidate for collecting air pollution dust derived from vehicles and (b) the potential inefficiencies involved in wiping the plant leaves are minimized by using wipe sheets, thus providing an effective method to study such pollution. Hoffmann et al. (1999) reported that the anthropogenic materials derived from passing traffic are deposited within 5 m with the peak concentration between 0 and 1 m from the roadside. Our results show the peak of SIRM intensity to be at 0 m at all sites except for site 16, where the peak appears at 0.5 m, with rapid intensity decay by 2 m. This result indicates that the anthropogenic pollutants do not travel far from the roadside into the surrounding wetland even though there are few trees to act as a barrier to the pollutants. Coastal areas along the Sea of Japan, including Mt. Tateyama, have been exposed to large amount of atmospheric acidic pollutants caused by Asian dust, which are delivered by the westerly jet stream and northwesterly

**Table 3** S-ratio of wipe paper samples

Distance from roadside (m)	Number of specimens	Averaged S-ratio	Standard deviation
0	12	0.99	0.01
0.5	9	0.99	0.00
1	10	1.00	0.01
1.5	2	1.00	–
2	10	0.99	0.00
3	3	0.98	–
4	2	1.00	–
5	10	0.99	0.01
6	1	0.99	–
10	5	0.97	0.02

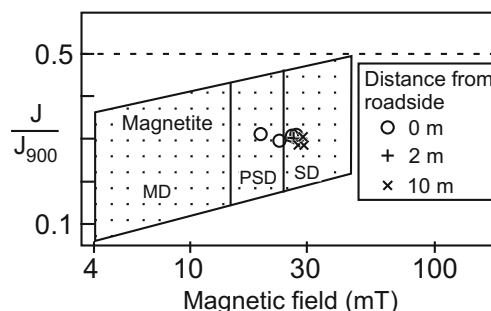


**Fig. 11** Crossover plots of selected samples. The magnetite-type plot of Symons and Cioppa (2000) is used since the coercivity of magnetite is close to the one of maghemite (Peters and Dekkers 2003)

winter monsoons (Nagashima et al. 2007; Watanabe et al. 2011). Such acidic pollutants could be the source of the observed magnetic minerals in the area (Kim et al. 2012). However, the similar spatial distributions of (a) the amounts of magnetic minerals, i.e., the higher SIRM intensities near the road side and its decrease with distance from the road, and (b) the grain size decreases with distance from the road as well as the distribution of heavy metal contents throughout the study area indicate that atmospheric acidic pollutants from long-range transportation from the Asian continent have little effect to the dust on the leaves in the area. In addition, lack of spherical grains implies that regional industrial processes such as the coal-fired/fuel oil-fired power plant at Toyama city located ~45 km northeast of Mt. Tateyama are minimal. Thus, this study shows that it would be reasonable to use magnetic parameters for estimating the spatial distribution of heavy metals from vehicular exhaust in Japan where environmental magnetic investigations on roadside pollution are usually avoided due to many active volcanoes and dense population (Torii 2005).

### Conclusions

Based on thermomagnetic remanence curves, low-temperature behaviors, SIRM acquisition tests, crossover plots, and Day plots, the main magnetic minerals in the leaf dust are coarse-grained magnetite with the presence of a superficial maghemite layer and SP minerals.

The in-field susceptibility measurements along the Tateyama Kurobe Alpine route at the Midagahara wetland area are similar in trend to the corresponding SIRM measurements from dust on dwarf bamboo leaves and to the previously reported results from the nearby Bijyodaira forest area. Our results show that in-field measurements are useful for estimating the spatial distribution of roadside dust even in a wetland area. *S. kurilensis*, or dwarf bamboo, are distributed in wide areas over East Asia, and they grow both adjacent to and far from the roads; i.e., these bamboo plants cover enough area to investigate the detailed spatial distribution of pollution.

The observed SIRM distributions show that the maximum intensities are adjacent to the roadside. Similarly, the closer the road, the higher the Fe, Pb, Cr, and Y concentrations observed. Therefore, the observed SIRM distributions and in-field susceptibility likely refer to the amounts of heavy metals. These results indicate that most of the pollutants are likely deposited within 2 m of the roadside at Mt. Tateyama. In addition, cross-over plots and Day plot analyses indicate that the magnetic grain size decreases with distance from the road, indicating that the main source of anthropogenic materials in the dust is likely delivered by passing vehicle rather than regional or faraway sources. Hence, the observed coarse magnetic minerals are likely formed by the oxidation of metallic Fe particle derived from vehicle exhaust. The universal distribution of Fe on analyzed grains by EPMA supports that the Fe is a suitable trace element for pollution investigation in the area.

Also, when the dust samples are prepared by wiping off the leaves with silica wool damped by ethanol, the samples are suitable for both high- and low-temperature experiments, allowing to identify not only magnetic mineralogy but also SP grain size that cannot be caught by a neodymium magnet. Wiping off the leaves' surface of dwarf bamboo with ethanol wipe sheet is a cheap, non-destructive, and effective method for collecting the dust deposited on leaves because the potential inefficiencies involved in wiping the plant surface are minimal. Therefore, the method should be considered for environmental magnetic application elsewhere where such bamboos or similar plant leaves are available.

**Acknowledgements** The authors gratefully thank Toyama District Forest Office for allowing access to the study area, Yoshitake Furuya for his help in field measurements and sampling, Dr. David Symons for helpful comments on an earlier draft of this manuscript, and anonymous reviewers for helpful comments that have improved this paper. This study was supported by a research grant from the Japan Seaology Promotion Organization through K.K.

**Compliance with ethical standards** This paper includes research involving neither human participants and/or animals, nor informed consent.

**Funding** This study was funded by the Japan Seaology Promotion Organization (Grant number: TIC-3).

**Conflict of interest** The authors declare that they have no conflict of interest.

## References

- Banin A, Ben-Shlomo T, Margulies L, Blake D, Mancinelli R, Gehring A (1993) The nanophase iron mineral (s) in Mars soil. *J Geophys Res: Planets* (1991–2012) 98:20831–20853
- Bloemendal J, King J, Hall F, Doh SJ (1992) Rock magnetism of Late Neogene and Pleistocene deep-sea sediments: relationship to sediment source, diagenetic processes, and sediment lithology. *J Geophys Res: Solid Earth* (1978–2012) 97:4361–4375
- de Boer CB, Dekkers MJ (1996) Grain-size dependence of the rock magnetic properties for a natural magnetite. *Geophys Res Lett* 23: 2815–2818
- Bučko MS, Magiera T, Pesonen LJ, Janus B (2010) Magnetic, geochemical, and microstructural characteristics of road dust on roadsides with different traffic volumes—case study from Finland. *Water Air Soil Pollut* 209:295–306
- Bučko MS, Magiera T, Johanson B, Petrovský E, Pesonen LJ (2011) Identification of magnetic particulates in road dust accumulated on roadside snow using magnetic, geochemical and micro-morphological analyses. *Environ Pollut* 159:1266–1276
- Bučko MS, Mattila O-P, Chrobak A, Ziolkowski G, Johanson B, Čuda J, Filip J, Zbořil R, Pesonen LJ, Leppäranta M (2013) Distribution of magnetic particulates in a roadside snowpack based on magnetic, microstructural and mineralogical analyses. *Geophys J Int* ggt 253
- Cambay M, Aydin A, Kurtulus C (2010) Magnetic susceptibility and heavy-metal contamination in topsoils along the Izmit Gulf coastal area and IZAYTAS (Turkey). *J Appl Geophys* 70:46–57
- Chevrier V, Mathé P-E, Rochette P, Gunnlaugsson HP (2006) Magnetic study of an Antarctic weathering profile on basalt: implications for recent weathering on Mars. *Earth Planet Sci Lett* 244:501–514
- Day R, Fuller M, Schmidt V (1977) Hysteresis properties of titanomagnetites: grain-size and compositional dependence. *Phys Earth Planet Inter* 13:260–267
- Desenfant F, Petrovský E, Rochette P (2004) Magnetic signature of industrial pollution of stream sediments and correlation with heavy metals: case study from South France. *Water Air Soil Pollut* 152: 297–312
- Dunlop DJ (2002a) Theory and application of the Day plot (Mrs/Ms versus Hcr/Hc) 1. Theoretical curves and tests using titanomagnetite data. *J Geophys Res* 107:EPM 4-1–EPM 4-22
- Dunlop DJ (2002b) Theory and application of the Day plot (Mrs/Ms versus Hcr/Hc) 2. Application to data for rocks, sediments, and soils. *J Geophys Res: Solid Earth* (1978–2012) 107:EPM 5-1–EPM 5-15
- Dunlop DJ, Özdemir Ö (1997) *Rock magnetism: fundamentals and frontiers*. Cambridge University Press, Cambridge
- Evans M, Heller F (2003) *Environmental magnetism: principles and applications of enviromagnetics*. Academic Press, New York, p 86
- Farmer AM (1993) The effects of dust on vegetation—a review. *Environ Pollut* 79:63–75
- Flanders PJ (1999) Identifying fly ash at a distance from fossil fuel power stations. *Environ Sci Technol* 33:528–532
- Gehring A, Fischer H, Louvel M, Kunze K, Weidler P (2009) High temperature stability of natural magnetite: a magnetic and spectroscopic study. *Geophys J Int* 179:1361–1371
- Grommé C, Wright T, Peck D (1969) Magnetic properties and oxidation of iron-titanium oxide minerals in Alae and Makaopuhi Lava Lakes, Hawaii. *J Geophys Res* 74:5277–5293
- Hansard R, Maher B, Kinnersley R (2012) Rapid magnetic biomonitoring and differentiation of atmospheric particulate pollutants at the roadside and around two major industrial sites in the UK. *Environ Sci Technol* 46:4403–4410
- Heller F, Strzyszczyk Z, Magiera T (1998) Magnetic record of industrial pollution in forest soils of upper Silesia, Poland. *J Geophys Res: Solid Earth* 103:17767–17774
- Herawati N, Suzuki S, Hayashi K, Rivai I, Koyama H (2000) Cadmium, copper, and zinc levels in rice and soil of Japan, Indonesia, and China by soil type. *Bull Environ Contam Toxicol* 64:33–39
- Hoffmann V, Knab M, Appel E (1999) Magnetic susceptibility mapping of roadside pollution. *J Geochem Explor* 66:313–326
- Hofman J, Stokkaer I, Snauwaert L, Samson R (2013) Spatial distribution assessment of particulate matter in an urban street canyon using biomagnetic leaf monitoring of tree crown deposited particles. *Environ Pollut* 183:123–132
- Horikawa K, Takeda M, Kawasaki K, Zhang J (2013) Historical changes in soil acidification inferred from the dendrochemistry of a



- Tateyama cedar at Bijodaira, Mt. Tateyama, Japan. *Geochem J* 47: 663–673
- Karimi R, Ayoubi S, Jalalian A, Sheikh-Hosseini AR, Afyuni M (2011) Relationships between magnetic susceptibility and heavy metals in urban topsoils in the arid region of Isfahan, central Iran. *J Appl Geophys* 74:1–7
- Kawano S (1999) Disturbance and conservation of the subalpine-alpine vegetation and biota in the Tateyama-Kurobe National Park, the Japan North Alps in Central Honshu, Japan—the results of long-term monitoring. *Jpn J Ecology* 49:313–320
- Kawasaki K, Horikawa K, Sakai H (2015) Environmental magnetism of roadside soil contamination in the restricted Bijyodaira area of Mt. Tateyama, Toyama, Japan. *Asian J Water Environ Pollut* 12:1–11
- Kim W, Doh S-J, Park Y-H, Yun S-T (2007) Two-year magnetic monitoring in conjunction with geochemical and electron microscopic data of roadside dust in Seoul, Korea. *Atmos Environ* 41:7627–7641
- Kim W, Doh S-J, Yu Y (2009) Anthropogenic contribution of magnetic particulates in urban roadside dust. *Atmos Environ* 43:3137–3144
- Kim W, Doh S-J, Yu Y (2012) Asian dust storm as conveyance media of anthropogenic pollutants. *Atmos Environ* 49:41–50
- Kletetschka G, Žila V, Wasilewski PJ (2003) Magnetic anomalies on the tree trunks. *Stud Geophys Geod* 47:371–379
- Kosterov A (2003) Low-temperature magnetization and AC susceptibility of magnetite: effect of thermomagnetic history. *Geophys J Int* 154:58–71
- Kume A, Numata S, Watanabe K, Honoki H, Nakajima H, Ishida M (2009) Influence of air pollution on the mountain forests along the Tateyama–Kurobe Alpine route. *Ecol Res* 24:821–830
- Lecoanet H, Lévêque F, Segura S (1999) Magnetic susceptibility in environmental applications: comparison of field probes. *Phys Earth Planet Inter* 115:191–204
- Lovley D, Moskowitz BM, Frankel RB, Bazylinski DA, Jannasch HW (1989) A comparison of magnetite particles produced anaerobically by magnetotactic and dissimilatory iron-reducing bacteria. *Geophys Res Lett* 16
- Lu S, Bai S (2006) Study on the correlation of magnetic properties and heavy metals content in urban soils of Hangzhou City, China. *J Appl Geophys* 60:1–12
- Lu S, Wang H, Guo J (2011) Magnetic enhancement of urban roadside soils as a proxy of degree of pollution by traffic-related activities. *Environmental Earth Sci* 64:359–371
- Maher BA, Moore C, Matzka J (2008) Spatial variation in vehicle-derived metal pollution identified by magnetic and elemental analysis of roadside tree leaves. *Atmos Environ* 42:364–373
- Matzka J, Maher BA (1999) Magnetic biomonitoring of roadside tree leaves: identification of spatial and temporal variations in vehicle-derived particulates. *Atmos Environ* 33:4565–4569
- Muxworthy A, Schmidbauer E, Petersen N (2002) Magnetic properties and Mössbauer spectra of urban atmospheric particulate matter: a case study from Munich, Germany. *Geophys J Int* 150:558–570
- Muxworthy AR, Matzka J, Davila AF, Petersen N (2003) Magnetic signature of daily sampled urban atmospheric particles. *Atmos Environ* 37:4163–4169
- Nagashima K, Tada R, Matsui H, Irino T, Tani A, Toyoda S (2007) Orbital- and millennial-scale variations in Asian dust transport path to the Japan Sea. *Palaeogeogr Palaeoclimatol Palaeoecol* 247:144–161
- Ninomiya J, Bergman W, Simpson B (1970) Automotive particulate emissions. In: Englund H (Hrsg.) 2nd International Clean Air Congress, International Union of Air Pollution Prevention Association, Washington, D. C., p 663–671
- Pandey SK, Tripathi B, Prajapati SK, Upadhyaya A, Mishra V, Rai PK, Sharma AP (2005) Magnetic properties of vehicle-derived particulates and amelioration by *Ficus infectoria*: a keystone species. *AMBIO: A J Human Environ* 34:645–647
- Peters C, Dekkers M (2003) Selected room temperature magnetic parameters as a function of mineralogy, concentration and grain size. *Physics and Chemistry of the Earth, Parts A/B/C* 28:659–667
- Petrovský E, Zbořil R, Grygar TM, Kotlík B, Novák J, Kapička A, Grison H (2013) Magnetic particles in atmospheric particulate matter collected at sites with different level of air pollution. *Stud Geophys Geod* 57:755–770
- Rai PK (2013) Environmental magnetic studies of particulates with special reference to biomagnetic monitoring using roadside plant leaves. *Atmos Environ* 72:113–129
- Rai PK, Chutia BM, Patil S (2014) Monitoring of spatial variations of particulate matter (PM) pollution through bio-magnetic aspects of roadside plant leaves in an Indo-Burma hot spot region. *Urban For Urban Green* 13:761–770
- Schadlich G, Weissflog L, Schuurmann G (1995) Magnetic susceptibility in conifer needles as indicator of fly ash deposition. *Fresenius Environ Bull* 4:7–12
- Schibler L, Boyko T, Ferdyn M, Gajda B, Höll S, Jordanova N, Rösler W, Team M (2002) Topsoil magnetic susceptibility mapping: data reproducibility and compatibility, measurement strategy. *Stud Geophys Geod* 46:43–57
- Schmidt A, Yamold R, Hill M, Ashmore M (2005) Magnetic susceptibility as proxy for heavy metal pollution: a site study. *J Geochem Explor* 85:109–117
- Spassov S, Heller F, Kretzschmar R, Evans M, Yue L, Nourgaliev D (2003) Detrital and pedogenic magnetic mineral phases in the loess/palaeosol sequence at Lingtai (Central Chinese Loess Plateau). *Phys Earth Planet Inter* 140:255–275
- Symons DTA, Cioppa MT (2000) Crossover plots: a useful method for plotting SIRM data in paleomagnetism. *Geophys Res Lett* 27:1779–1782
- Tauxe L (1998) *Paleomagnetic principles and practice*, 17. Kluwer Academic Publishers, Dordrecht
- Thompson J, Mueller P, Flückiger W, Rutter A (1984) The effect of dust on photosynthesis and its significance for roadside plants. *Environ Pollut Series A, Ecol Biol* 34:171–190
- Tong Y, Li A, Cai Y, Ni X, Zhang Y, Wang J, Guo P, Li X, Zhang G (2001) Mössbauer study of atmospheric aerosols of Shanghai. *Environ Sci Technol* 35:1432–1436
- Torii M (2005) Environmental magnetism: a brief review. *J Geogr* 114: 284–295
- Versteeg JK, Morris WA, Rukavina NA (1995) The utility of magnetic properties as a proxy for mapping contamination in Hamilton Harbour sediment. *J Great Lake Res* 21:71–83
- Wang XS, Yong Q (2005) Correlation between magnetic susceptibility and heavy metals in urban topsoil: a case study from the city of Xuzhou, China. *Environ Geol* 49:10–18
- Wang B, Xia D, Yu Y, Jia J, Xu S (2013) Magnetic records of heavy metal pollution in urban topsoil in Lanzhou, China. *Chin Sci Bull* 58:384–395
- Watanabe K, Saito Y, Tamura S, Sakai Y, Eda N, Aoki M, Kawabuchi M, Yamada H, Iwai A, Kawada K (2011) Chemical characteristics of the snow pits at Murododaira, Mount Tateyama, Japan. *Ann Glaciol* 52:102–110
- Weber S, Hoffmann P, Enslin J, Dedik A, Weinbruch S, Mieke G, Gütlich P, Ortner H (2000) Characterization of iron compounds from urban and rural aerosol sources. *J Aerosol Sci* 31:987–997
- Yang T, Liu Q, Li H, Zeng Q, Chan L (2010) Anthropogenic magnetic particles and heavy metals in the road dust: magnetic identification and its implications. *Atmos Environ* 44:1175–1185
- Zhang C, Huang B, Piper JD, Luo R (2008) Biomonitoring of atmospheric particulate matter using magnetic properties of *Salix matsudana* tree ring cores. *Sci Tot Environ* 393:177–190
- Zhang C, Qiao Q, Appel E, Huang B (2012) Discriminating sources of anthropogenic heavy metals in urban street dusts using magnetic and chemical methods. *J Geochem Explor* 119:60–75